

Anisotropic perturbations in three-dimensional $O(N)$ -symmetric vector models

Martin Hasenbusch*

Institut für Physik, Humboldt-Universität zu Berlin, Newtonstrasse 15, D-12489 Berlin, Germany

Ettore Vicari†

Dipartimento di Fisica dell'Università di Pisa and INFN, I-56127 Pisa, Italy

(Received 5 August 2011; published 29 September 2011)

We investigate the effects of anisotropic perturbations in three-dimensional $O(N)$ -symmetric vector models. In order to assess their relevance for the critical behavior, we determine the renormalization-group dimensions of the anisotropic perturbations associated with the first few spin values of the representations of the $O(N)$ group, because the lowest spin values give rise to the most important effects. In particular, we determine them up to spin 4 for $N = 2, 3, 4$, by finite-size analyses of Monte Carlo simulations of lattice $O(N)$ models, achieving a significant improvement of their accuracy. These results are relevant for several physical systems, such as density-wave systems, magnets with cubic symmetry, and multicritical phenomena arising from the competition of different order parameters.

DOI: [10.1103/PhysRevB.84.125136](https://doi.org/10.1103/PhysRevB.84.125136)

PACS number(s): 05.70.Jk, 64.60.F-, 05.10.Cc

I. INTRODUCTION AND SUMMARY

Many continuous phase transitions observed in nature belong to the $O(N)$ vector universality classes, which are characterized by an N -component order parameter with $O(N)$ symmetry and the symmetry breaking $O(N) \rightarrow O(N-1)$. The superfluid transition in ^4He , the formation of Bose-Einstein condensates, density wave systems, transitions in magnets with easy-plane anisotropy, and in superconductors belong to the XY or $O(2)$ universality class; the Curie transition in isotropic magnets, zero-temperature quantum transitions in two-dimensional antiferromagnets, are examples for the Heisenberg or $O(3)$ universality class; the $O(4)$ universality class is relevant for the finite-temperature transition in two-flavor quantum chromodynamics, the theory of strong interactions. See, for example, Refs. 1 and 2 for reviews.

In the absence of external fields, the phase transition of $O(N)$ -symmetric vector models is driven by only one relevant parameter, which is usually associated with the temperature. The corresponding RG dimension is $y_t = 1/\nu$ where ν is the correlation-length exponent. The leading odd perturbation, which breaks the $O(N)$ symmetry, is associated with the external field h coupled to the order parameter; it has RG dimension $y_h = (d+2-\eta)/2$, where η is the exponent controlling the power-law space dependence of the two-point correlation function of the order parameter at criticality. The asymptotic critical power-law behaviors of $O(N)$ -symmetric vector models have been determined with high accuracy. In Table I we report some of the most accurate estimates of the critical exponents ν and η , and of the leading and next-to-leading scaling-correction exponents ω and ω_2 , which characterize the dominant corrections to the universal scaling.

In this paper we study the effects of anisotropic perturbations breaking the $O(N)$ symmetry, which cannot be related to an external vector field coupled to the order parameter, but which are represented by composite operators with more complex transformation properties under the $O(N)$ group. An interesting question is whether they change the critical behavior, or whether they do not affect it so that the symmetry

shown by the critical correlations is larger than that of the microscopic model. This issue arises in several physical contexts. Anisotropy in magnetic systems may naturally arise due to the cubic structure of the underlying lattice, giving rise to anisotropic interactions terms (see, e.g., Ref. 12). The relevance of the anisotropic perturbations determines also the nature of the multicritical behavior at the meeting point of two transition lines with different $O(n_1)$ and $O(n_2)$ symmetries, in particular, whether the symmetry gets effectively enlarged to $O(n_1+n_2)$ (see, e.g., Refs. 11, 13, and 14). Another interesting issue is the critical behavior of secondary order parameters, which are generally represented by powers of the order parameter transforming as higher representations of the $O(N)$ group; their critical behaviors can be measured in density wave systems, such as liquid crystals^{15–17} (see also Refs. 18–21).

Let us consider the general problem of the $O(N)$ -symmetric theory in the presence of an external field h_p coupled to a perturbation P . Assuming P to be an eigenoperator of the RG transformations, the singular part of the free energy for the reduced temperature $t \rightarrow 0$ and $h_p \rightarrow 0$ can be written as

$$F_{\text{sing}} = |t|^{d\nu} f(h_p/|t|^{y_p\nu}), \quad (1)$$

where y_p is the RG dimension of h_p , and $f(x)$ is a scaling function. Therefore, the RG dimensions of the anisotropic external fields quantitatively control their capability to influence or change the asymptotic critical behavior when $y_p > 0$.

In the field-theoretical (FT) framework the $O(N)$ -symmetric vector model is represented by the $O(N)$ -symmetric Landau-Ginzburg-Wilson theory

$$\mathcal{H} = \int d^d x \left[\frac{1}{2}(\partial_\mu \Phi)^2 + \frac{1}{2}r\Phi^2 + \frac{1}{4!}u(\Phi^2)^2 + h \cdot \Phi \right], \quad (2)$$

where Φ is an N -component real field and h an external field. The anisotropic perturbations are conveniently classified^{2,22} using irreducible representations of the $O(N)$ internal group, characterized by the spin value l . Let us consider the perturbation $P_{m,l}$ defined by the power m of the order parameter and the spin representation l of the $O(N)$ group

$$P_{m,l}^{a_1 \dots a_l}(\Phi) = (\Phi^2)^{(m-l)/2} \mathcal{Q}_l^{a_1 \dots a_l}(\Phi), \quad (3)$$

TABLE I. Some of the most accurate results for the critical exponents of the three-dimensional $O(N)$ vector universality classes with $N = 2, 3, 4, 5$. We report estimates of ν and η , and of the leading and next-to-leading scaling correction exponents, obtained by lattice techniques (LT) based on Monte Carlo simulations and/or high-temperature expansions, and by quantum field theory (FT) techniques such as high-order perturbative expansions. The results without reference have been obtained in this paper. A more complete review of results can be found in Ref. 2.

N	Method	ν	η	ω	ω_2
2	LT	0.6717(1) ³	0.0381(2) ³	0.785(20) ³	
	FT	0.6703(15) ⁴	0.0354(25) ⁴	0.789(11) ⁴	1.77(7) ⁵
3	LT	0.7112(5) ⁶	0.0375(5) ⁶	0.773 ⁸	
		0.7117(5) ⁷	0.0378(5) ⁷		
		0.7116(10)	0.0378(3)		
4	FT	0.7073(35) ⁴	0.0355(25) ⁴	0.782(13) ⁴	1.78(11) ⁵
	LT	0.749(2) ⁸	0.0365(10) ⁸	0.765 ⁸	
5		0.7477(8) ⁹	0.0360(4) ⁹		
		0.750(2)	0.0360(3)		
	FT	0.741(6) ⁴	0.0350(45) ⁴	0.774(20) ⁴	
5	LT	0.779(3) ¹⁰	0.034(1) ¹⁰		
	FT	0.762(7) ¹¹	0.034(4) ¹¹	0.790(15) ¹¹	

where $Q_l^{a_1 \dots a_l}$ is a homogeneous polynomial of degree l that is symmetric and traceless in the l indices:

$$Q_1^a(\Phi) = \Phi^a, \quad (4)$$

$$Q_2^{ab}(\Phi) = \Phi^a \Phi^b - \frac{1}{N} \delta^{ab} \Phi^2, \quad (5)$$

$$Q_3^{abc}(\Phi) = \Phi^a \Phi^b \Phi^c - \frac{\Phi^2}{N+2} (\Phi^a \delta^{bc} + \Phi^b \delta^{ac} + \Phi^c \delta^{ab}),$$

$$Q_4^{abcd}(\Phi) \quad (6)$$

$$= \Phi^a \Phi^b \Phi^c \Phi^d - \frac{1}{N+4} \Phi^2 (\delta^{ab} \Phi^c \Phi^d + \delta^{ac} \Phi^b \Phi^d + \delta^{ad} \Phi^b \Phi^c + \delta^{bc} \Phi^a \Phi^d + \delta^{bd} \Phi^a \Phi^c + \delta^{cd} \Phi^a \Phi^b) + \frac{1}{(N+2)(N+4)} (\Phi^2)^2 (\delta^{ab} \delta^{cd} + \delta^{ac} \delta^{bd} + \delta^{ad} \delta^{bc}), \quad (7)$$

etc. The classification in terms of spin values is particularly convenient: (i) under the RG flow the operators with different spin never mix; (ii) all parameters $h_{m,l}^{a_1 \dots a_l}$ associated with the components of $P_{m,l}^{a_1 \dots a_l}$ have the same RG dimension $Y_{m,l}$. On the other hand, operators with different m but with the same l mix under renormalization.

The spin-0 operators are already present in the Φ^4 Hamiltonian (2): the RG dimension of $P_{2,0}$ is related to the correlation length exponent $Y_{2,0} = y_t = 1/\nu$, while the RG dimension of $P_{4,0}$ (after an appropriate subtraction to cancel the mixing with $P_{2,0}$) gives the leading scaling correction exponent, indeed $Y_{4,0} = -\omega$. The spin-1 perturbation is related to the external field coupled to the order parameter, thus $Y_{1,1} = y_h$. (The perturbation $P_{3,1}^a$ is redundant²³ because a Hamiltonian term containing $P_{3,1}$ can be always eliminated by a redefinition of the field Φ^a . Anyway, using the equation of motion, one obtains $Y_{3,1} = (d-2+\eta)/2$.) Close to four dimensions, thus for small $\epsilon \equiv 4-d$, $Y_{m,l} < 0$ for $l \geq 5$, which implies that the only relevant operators have $l \leq 4$. It is reasonable to assume that this property holds up to $d = 3$. Moreover, near four

dimensions we can use standard power counting to verify that the perturbation with indices m,l mixes with $P_{m',l}$, $m' \leq m$, but their RG dimensions are significantly smaller. In principle, one should also consider terms with derivatives of the field, but again one can show that they are all irrelevant or redundant.

The above arguments show that the most interesting anisotropic perturbations are represented by the spin-2, spin-3, and spin-4 operators

$$Q_2^{ab} = P_{2,2}^{ab}, \quad Q_3^{abc} = P_{3,3}^{abc}, \quad Q_4^{abcd} = P_{4,4}^{abcd}, \quad (8)$$

because they provide the leading effects of anisotropy for each spin sector. As we shall see, the leading RG dimensions within each spin sector,

$$Y_l \equiv Y_{l,l}, \quad (9)$$

characterize interesting critical behaviors in various physical contexts. Some Y_l have been already estimated by using FT approaches based on high-order perturbative calculations, and lattice techniques, such as high-temperature (HT) expansions and Monte Carlo (MC) simulations. In Table II we report some results for $N = 2, 3, 4, 5$. In most cases these results already provide a clear indication of the relevance of the perturbation, with the only exception of the spin-4 perturbation in the $O(3)$ universality class, where the value of Y_4 is close to zero. While high-order FT results indicate the relevance of the spin-4 perturbation, the MC estimate of Y_4 appears compatible with zero. Since the issue concerning its relevance is of experimental interest, an accurate determination of Y_4 is called for to conclusively settle it.

In this paper we present new accurate estimates of the RG dimensions Y_l of the anisotropic perturbations for $N = 2, 3, 4$. For this purpose we perform finite-size scaling (FSS) analyses of Monte Carlo (MC) simulations of lattice $O(N)$ spin systems. We achieve a significant improvement of the accuracy of the estimates of Y_l , essentially by combining the FSS method of Ref. 24 with the use of improved Hamiltonians,²⁸ which are characterized by the fact that the leading correction to scaling is suppressed in the asymptotic expansion of any observable near the critical point. Our results are also reported in Table II. As we shall explain later, the errors in the estimates of Y_l , and in particular of Y_4 , are quite prudential, they are largely dominated by the systematic error arising from the necessary truncation of the Wegner expansions²² which provide the asymptotic FSS behavior of the quantities considered. The results are a good agreement with the estimates obtained by the analyses of high-order FT perturbative expansions, in particular with those obtained by resumming sixth-order $d = 3$ expansions. Our results show that spin-4 perturbations in three-dimensional Heisenberg systems are relevant, with a quite small RG dimension $Y_4 = 0.013(4)$, which may give rise to very slow crossover effects in systems with small spin-4 anisotropy. The apparent discrepancy with the MC result of Ref. 24, obtained using the standard nearest-neighbor $O(3)$ spin model, can be explained by the presence of sizable scaling corrections. We overcome this problem by using improved lattice Hamiltonians. The relevance of the spin-4 perturbations is important for systems with cubic perturbations,¹² and also systems whose phase diagram presents two transition lines,

TABLE II. Estimates of the RG dimensions Y_l of the couplings h_l associated with the leading anisotropic perturbations Q_l for the three-dimensional $O(N)$ vector universality classes with $N = 2, 3, 4, 5$. We report results obtained by various methods, such as FT perturbative expansions within $d = 3$ and ϵ -expansion schemes, and lattice techniques, such as high-temperature expansions (HT) and finite-size scaling analyses of Monte Carlo simulations (FSS MC). Notice that in the MC estimates of Y_4 reported in Ref. 24 only statistical errors are explicitly given; the authors write that systematic errors are likely of a similar size.

N	Method	Y_2 (spin 2)	Y_3 (spin 3)	Y_4 (spin 4)
2	FT fifth-order ϵ expansion	1.766(6) ¹¹	0.90(2) ²⁵	-0.114(4) ²⁶
	FT sixth-order $d = 3$ expansion	1.766(18) ¹¹	0.897(15) ²⁵	-0.103(8) ²⁶
	HT	1.75(2) ²⁷		
	FSS MC			-0.171(17) ²⁴
	FSS MC (this paper)	1.7639(11)	0.8915(20)	-0.108(6)
3	FT fifth-order ϵ expansion	1.790(3) ¹¹	0.96(3) ²⁵	0.003(4) ²⁶
	FT sixth-order $d = 3$ expansion	1.80(3) ¹¹	0.97(4) ²⁵	0.013(6) ²⁶
	HT	1.76(2) ²⁷		
	FSS MC			-0.0007(29) ²⁴
	FSS MC (this paper)	1.7906(3)	0.9616(10)	0.013(4)
4	FT fifth-order ϵ expansion	1.813(6) ¹¹	1.04(5) ²⁵	0.105(6) ²⁶
	FT sixth-order $d = 3$ expansion	1.82(5) ¹¹	1.03(3) ²⁵	0.111(4) ²⁶
	FSS MC			0.1299(24) ²⁴
	FSS MC (this paper)	1.8145(5)	1.0232(10)	0.125(5)
5	FT fifth-order ϵ expansion	1.832(8) ¹¹	1.08(4) ²⁵	0.198(11) ¹¹
	FT sixth-order $d = 3$ expansion	1.83(5) ¹¹	1.07(2) ²⁵	0.189(10) ¹¹
	FSS MC			0.23(2) ¹⁰

XY and Ising transition lines, meeting at a multicritical point.¹³ We shall further discuss these physical applications later.

The remainder of the paper is organized as follows. In Sec. II we present the lattice ϕ^4 model which we consider in our MC simulations, and provide the definitions of the quantities that we consider in our FSS analyses, in particular, those related to the spin- l anisotropies. In Sec. III we describe our FSS analyses of MC simulations which lead to our final estimates already reported in Table II. Finally, in the conclusive Sec. IV we discuss a number of physical applications of our results. Appendices A and B contain some details of the MC simulations, and further results on the critical behavior of $O(N)$ vector models.

II. THE LATTICE MODEL AND THE ESTIMATORS OF THE ANISOTROPY RG DIMENSIONS

A. Improved lattice $O(N)$ -symmetric ϕ^4 models

In this numerical study of $O(N)$ vector models with $N = 2, 3, 4$, we consider the ϕ^4 $O(N)$ -symmetric lattice Hamiltonian

$$\mathcal{H}_{\phi^4} = -\beta \sum_{\langle xy \rangle} \phi_x \cdot \phi_y + \sum_x [\phi_x^2 + \lambda(\phi_x^2 - 1)^2], \quad (10)$$

where ϕ_x is an N -component real variable, x and y denote sites of the simple-cubic lattice, and $\langle xy \rangle$ is a pair of nearest-neighbor sites. In our convention, the Boltzmann factor is given by $\exp(-\mathcal{H}_{\phi^4})$. For $\lambda = 0$ we get the Gaussian model, while in the limit $\lambda \rightarrow \infty$ the $O(N)$ -symmetric nonlinear σ model is recovered. For any $0 < \lambda \leq \infty$ the model undergoes a continuous phase transition in the universality class of the $O(N)$ -symmetric vector model.

In our FSS analyses we consider cubic L^3 lattices with periodic boundary conditions. We consider standard finite-volume quantities such as the magnetic susceptibility and second-moment correlation length related to the two-point function $G(x - y) \equiv \langle \phi_x \cdot \phi_y \rangle$, that is,

$$\chi \equiv \frac{1}{L^3} \langle M^2 \rangle, \quad M = \sum_x \phi_x, \quad (11)$$

and

$$\xi \equiv \sqrt{\frac{\chi/F - 1}{4 \sin^2 \pi/L}}, \quad F \equiv \frac{1}{L^3} \left\langle \left| \sum_x \exp\left(i \frac{2\pi x_1}{L}\right) \phi_x \right|^2 \right\rangle. \quad (12)$$

Another standard quantity for FSS analyses is the quartic Binder cumulant

$$U_4 \equiv \frac{\langle (M^2)^2 \rangle}{\langle M^2 \rangle^2}. \quad (13)$$

The ratio ξ/L and U_4 are RG-invariant phenomenological couplings, thus their large-volume limit at T_c is universal. We also consider quantities defined keeping one of the phenomenological coupling fixed, in particular keeping the ratio ξ/L fixed (see, e.g., Ref. 29). We define \tilde{U}_4 as the Binder cumulant at fixed ξ/L . (In previous studies (see Refs. 3, 6, and 29) another RG-invariant quantity turned out to be very useful, i.e., the ratio Z_a/Z_p of partition functions of a system with antiperiodic boundary conditions in one direction and periodic ones in the other two directions and a system with periodic boundary conditions in all directions. Since here we focus on the anisotropy, we have not implemented it to keep the project manageable.)

Improved Hamiltonians are characterized by the fact that the leading correction to scaling is eliminated in any quantity near the critical point. Therefore in a MC study, the asymptotic behavior at the phase transition can be determined more precisely. Improved Hamiltonians were first discussed in Ref. 28 for the three-dimensional Ising universality class using high-temperature series expansions. This idea was first implemented in MC simulations of ϕ^4 $O(N)$ -symmetric lattice models for $N = 2, 3$, and 4 in Refs. 8 and 30. In the case of the ϕ^4 lattice model (10), the improved model is obtained by tuning the parameter λ to the particular value λ^* , where the leading $O(L^{-\omega})$ scaling corrections vanish in the FSS behavior of any quantity. For this purpose, the RG-invariant phenomenological couplings turn out to be particularly useful. Indeed, along the critical line $\beta_c(\lambda)$ or keeping another phenomenological coupling constant, they behave as

$$R(L, \lambda) = R^* + c(\lambda)L^{-\omega} + \dots, \quad (14)$$

where $c(\lambda)$ is a smooth function of λ . Therefore, the equation $c(\lambda^*) = 0$ determines λ^* .

The best estimate of λ^* for $N = 2$ is $\lambda^* = 2.15(5)$ obtained in Ref. 3. In the case of $N = 3, 4$, the MC simulations performed for this numerical work lead to a revision of the earlier estimates of λ^* , see Appendix B for details. We obtain $\lambda^* = 5.2(4)$ for $N = 3$ and $\lambda^* = 20_{-6}^{+15}$ for $N = 4$, which update earlier estimates, respectively, $\lambda^* = 4.6(4)$ of Ref. 6 and $\lambda^* = 12.5(4.0)$ of Ref. 8.

B. Anisotropy estimators

In order to compute the spin- l RG dimensions Y_l , we consider appropriate anisotropy correlators. We use the magnetization $M^a = \sum_x \phi_x^a$ and the normalized magnetization m^a defined as

$$m^a \equiv \frac{M^a}{|M|} \quad (15)$$

to construct objects with given spin properties, such as $Q_2^{ab}(m)$, $Q_3^{abc}(m)$, and $Q_4^{abcd}(m)$, obtained by replacing Φ^a with m^a in the expressions of Q_l [cf. Eqs. (5)–(7)]. Then we consider the correlators

$$C_2 = \sum_{ab} \left\langle \sum_x Q_2^{ab}(\phi_x) Q_2^{ab}(m) \right\rangle, \quad (16)$$

$$C_3 = \sum_{abc} \left\langle \sum_x Q_3^{abc}(\phi_x) Q_3^{abc}(m) \right\rangle, \quad (17)$$

$$C_4 = \sum_{abcd} \left\langle \sum_x Q_4^{abcd}(\phi_x) Q_4^{abcd}(m) \right\rangle, \quad (18)$$

where $Q_l(\phi_x)$ are the operators (5)–(7) constructed using the lattice variable ϕ_x^a . Note that they can be rewritten in term of the angle α_x defined as $\phi_x \cdot m = |\phi_x| \cos \alpha_x$, as

$$C_2 = \left\langle \sum_x |\phi_x|^2 \left(\cos^2 \alpha_x - \frac{1}{N} \right) \right\rangle,$$

$$C_3 = \left\langle \sum_x |\phi_x|^3 \left(\cos^3 \alpha_x - \frac{3}{N+2} \cos \alpha_x \right) \right\rangle,$$

$$C_4 = \left\langle \sum_x |\phi_x|^4 \left[\cos^4 \alpha_x - \frac{6}{N+4} \cos^2 \alpha_x + \frac{3}{(N+2)(N+4)} \right] \right\rangle.$$

This expression of C_4 shows that it is equal to the improved quantity considered in Ref. 24 to compute the RG dimension of the cubic-symmetric perturbation, apart from a constant factor. The asymptotic power-law FSS behavior of C_l at T_c , that is,

$$C_l \sim L^{Y_l}, \quad (19)$$

allows us to estimate the RG dimension Y_l of the anisotropy associated with Q_l . Alternative estimators analogous to C_l are also

$$D_l = \sum_{ab\dots} \frac{\langle \sum_x Q_l^{ab\dots}(\phi_x) Q_l^{ab\dots}(M) \rangle}{\langle M^2 \rangle^{l/2}}, \quad D_l \sim L^{Y_l}. \quad (20)$$

Note that $\langle Q_l^{ab\dots}(m) \rangle$ and $\langle Q_l^{ab\dots}(M) \rangle / \langle M^2 \rangle^{l/2}$ are by construction RG-invariant quantities (with special symmetry properties). Their derivatives with respect to h_p [cf. Eq. (1)] provide the correlators C_l and D_l . We also consider the corresponding quantities \tilde{C}_l and \tilde{D}_l at a fixed value of ξ/L .

III. FSS ANALYSES OF THE ANISOTROPY CORRELATORS

In this section we present FSS analyses of high-statistics MC simulations for the $O(2)$, $O(3)$, and $O(4)$ ϕ^4 lattice models (10) for values of the parameter λ close to λ^* providing the suppression of the leading scaling correction. Appendix A 1 presents some details of the MC algorithm used in the simulations; Appendix A 2 reports the values of the parameters considered in our MC simulations, the lattice sizes, and the statistics; finally in Appendix A 3 we discuss the behavior of the variance of the observables considered, which influenced the strategy of our FSS analyses of MC simulations.

Most simulations were performed for the $O(3)$ case, where the spin-4 RG dimension Y_4 is close to zero, and therefore high accuracy is needed to determine its sign. This task is made particularly hard by the rapid increase of the cost to get accurate data for C_4 and D_4 with increasing the lattice size, essentially due to a significant increase of their variance (see the discussion in Appendix A 3). As a consequence, our FSS analyses to determine Y_4 are limited to relatively small lattice sizes. On the other hand, the systematic error due to the necessary truncation of the Wegner expansion²² [see Eq. (21) below] of the quantities considered turns out to be significant, and its reduction requires accurate results for large lattice sizes. This represents the major limitation for the accuracy of our numerical determination of Y_4 .

Appendix B reports further FSS analyses of the MC simulations which allow us to update some of the results concerning the $O(N)$ vector models, such as the estimates of λ^* , of the critical exponents and other universal quantities.

A. General strategy of the FSS analysis

In order to obtain accurate estimates of the universal quantities, such as the critical exponents and RG dimensions

Y_l , it is important to have a robust control of the corrections to the asymptotic behaviors, which are suppressed by powers of the lattice size L . The behavior of general quantities introduced to estimate critical exponents, such as C_l and D_l defined in the previous section, can be expressed by an asymptotic Wegner expansion²² as

$$A(\lambda; L) = c(\lambda)L^y \left[1 + a(\lambda)L^{-\omega} + \sum_{i=2} a_i(\lambda)L^{-\omega_i} \right], \quad (21)$$

where y is the leading universal exponent that one wants to accurately estimate. In the case of $O(2)$, $O(3)$, and $O(4)$ vector models the leading scaling correction exponent is given by $\omega \approx 0.8$ (see Table I). Numerical approaches based on improved Hamiltonians allow us to suppress these leading scaling corrections, and also those related to $n\omega$, where $n = 2, 3, 4, \dots$, whose coefficients behave as $(\lambda - \lambda^*)^n$. The next-to-leading correction is controlled by the exponent ω_2 , estimated in Ref. 5 by $\omega_2 \approx 1.8$ (see Table I). Then there are well established corrections with $\omega_i \approx 2$, for example related to the breaking of spatial rotational invariance in cubic lattice systems,³¹ but also to analytic backgrounds, etc. Moreover, in the case of the spin- l anisotropy correlators, we may also have scaling corrections induced by higher-dimensional spin- l operators, such as $P_{l+2,l}$ [cf. Eq. (3)]. On the basis of a dimensional analysis around four dimensions, they are expected to give rise to scaling corrections suppressed by powers $\kappa_l = 2 + O(\epsilon)$, as also shown by the $O(\epsilon)$ calculation of the difference of the RG dimensions of the anisotropy operators $P_{l+2,l}$ and $P_{l,l}$, which is (We note that within ϵ expansion the operator $P_{l+2,l}$ mixes with other spin- l operators containing derivatives (two derivatives instead of Φ^2), but this mixing contributes to $O(\epsilon^2)$.)

$$Y_{l+2,l} - Y_{l,l} = -2 - \epsilon 6(l-1)/(N+8) + O(\epsilon^2). \quad (22)$$

In known cases for the spin-0,1,2 sectors, the difference between RG dimensions of the same sector remains close to their four-dimensional values. Therefore, as a prudential procedure, after curing the residual $O(L^{-\omega})$ scaling corrections, see also below, we must consider possible $O(L^{-\kappa})$ scaling corrections with $\kappa \gtrsim 1.6$.

1. Residual leading scaling corrections in approximately improved Hamiltonians

Residual leading scaling corrections are generally present due to the fact that λ^* is only known approximately, and also because the MC simulations are usually performed close but not exactly at the best estimate of λ^* , which is usually determined at the end of the MC simulations. For example, in the case $N = 3$ our best estimate is $\lambda^* = 5.2(4)$, while most MC simulations were performed at $\lambda = 4.5$, and others at $\lambda = 4$ and $\lambda = 5$ for smaller lattices to determine λ^* .

The residual $O(L^{-\omega})$ corrections, due to the fact that λ is close but does not coincide with its optimal value λ^* , can be further suppressed as follows. The basic idea is that leading corrections to scaling can be best detected by analyzing the Binder cumulant \bar{U}_4 at a fixed value of ξ/L . At a generic $\lambda = \lambda_0$ we have

$$\bar{U}_4(\lambda_0; L) = \bar{U}_4^* + a_U(\lambda_0)L^{-\omega} + \dots, \quad (23)$$

where \bar{U}_4^* is the universal large-volume limit on a periodic L^3 box at fixed ξ/L , which of course depends on which value of ξ/L is chosen. Then, we consider a pair λ_1, λ_2 , where one of the two values may be equal to λ_0 , and the differences

$$\Delta_U(\lambda_1, \lambda_2; L) = \bar{U}_4(\lambda_2; L) - \bar{U}_4(\lambda_1; L), \quad (24)$$

where the leading large-volume contributions cancel, thus they behave as

$$\Delta_U(\lambda_1, \lambda_2; L) = b_U(\lambda_1, \lambda_2)L^{-\omega} + \dots \quad (25)$$

The amplitude $b_U(\lambda_1, \lambda_2) = a_U(\lambda_2) - a_U(\lambda_1)$ can be estimated by fitting the data to (25). Finally, we take ratios

$$r_A(\lambda_1, \lambda_2; L) = \frac{A(\lambda_2; L)}{A(\lambda_1; L)} \quad (26)$$

of the quantity A that we intend to correct to eliminate the residual $O(L^{-\omega})$ corrections. Their data can be fitted to its large- L behavior

$$r_A(\lambda_1, \lambda_2; L) = \frac{c(\lambda_2)}{c(\lambda_1)} [1 + b(\lambda_1, \lambda_2)L^{-\omega}], \quad (27)$$

where $b(\lambda_1, \lambda_2) = a(\lambda_2) - a(\lambda_1)$ and $a(\lambda)$ is the amplitude of the $O(L^{-\omega})$ corrections [cf. Eq. (21)]. Notice that it is simpler to extract $b(\lambda_1, \lambda_2)$ than $a(\lambda)$ from the numerical data because, beside the cancellation of the power divergence L^y , also subleading corrections cancel to a large extent. Now we use the universality of ratios of correction amplitudes, which implies

$$\frac{a(\lambda_0)}{a_U(\lambda_0)} = \frac{b(\lambda_1, \lambda_2)}{b_U(\lambda_1, \lambda_2)}. \quad (28)$$

In order to eliminate the leading $O(L^{-\omega})$ corrections from A , we construct

$$\mathcal{I}_A(\lambda_0; L) = A(\lambda_0; L) \left[1 - \frac{b(\lambda_1, \lambda_2)}{b_U(\lambda_1, \lambda_2)} a_U(\lambda_0)L^{-\omega} \right]. \quad (29)$$

This procedure eliminates the leading $O(L^{-\omega})$ scaling corrections, allowing us to neglect them in the fits of the data of $\mathcal{I}_A(\lambda_0; L)$ to estimate the leading exponent y . (The coefficient $c \equiv a_U(\lambda_0)b(\lambda_1, \lambda_2)/b_U(\lambda_1, \lambda_2)$ is numerically determined with an error Δc , which is usually dominated by the uncertainty on $a_U(\lambda_0)$. This error can be taken into account by computing $\mathcal{I}_A(\lambda_0; L)$ using c and $c \pm \Delta c$. The difference between the results of their fits is essentially related to the error due to the uncertainty of our estimate for λ^* , since also the uncertainty of the estimate of λ^* is mainly caused by the error of $a_U(\lambda_0)$ (see also Appendix B 2).)

We also mention that alternative procedures, based on the idea of defining improved observables with suppressed leading scaling corrections, are outlined in Refs. 3 and 32.

2. Next-to-leading corrections

Next-to-leading corrections arise from the term associated with $\omega_2 \approx 1.8$, and the others with exponents close to two. In the fits of the data, even with high statistics data as we have here, only a very limited number of correction terms can be taken into account. The truncation of Eq. (21) leads to systematic errors in the results for the exponent y .

One way to control these systematic errors is to study several quantities $A^{(n)}$ that have the same critical behavior:

$$A^{(n)}(L) = c_n L^y \left(1 + \sum_i a_{ni} L^{-\omega_i} \right). \quad (30)$$

In general one might expect that for different $A^{(n)}$ the coefficients a_{ni} are different. Therefore the variation of the estimate for y obtained by fitting several $A^{(n)}$ provides an estimate of the systematic error. However, in our case we have only the two quantities C_l and D_l , which are closely related. Therefore we would like to estimate the systematic error by fitting a single quantity. To this end we consider the ansatz

$$A(L) = cL^y(1 + aL^{-\omega} + a_{2,\text{eff}}L^{-\omega_{2,\text{eff}}}) \quad (31)$$

(for improved models $a = 0$) with

$$\omega_{2,\text{eff}} \geq 1.6. \quad (32)$$

Barring an unlike significant cancellation between different correction terms, there must be a value of $\omega_{2,\text{eff}} > 1.6$ such that y takes its correct value. Since we expect that as long as correction are small the resulting y is a monotonic function of $\omega_{2,\text{eff}}$, we use the results obtained for $\omega_{2,\text{eff}} = 1.6$ and $\omega_{2,\text{eff}} = \infty$ (i.e., without the term $c_{2,\text{eff}}L^{-\omega_{2,\text{eff}}}$) as bounds for the correct result for y .

B. Results for the spin- l RG dimensions

1. The $O(3)$ model

To begin with we present the FSS analysis of the data for the $O(3)$ model. In order to give an idea of the quality of our data, we show the data of C_l at β_c and $\lambda = 4.5$ in Figs. 1 and 2. In all cases, including C_4 , the data clearly increase with increasing L , indicating the relevance of the perturbation. Note that the error of C_4 is rapidly increasing with increasing L (see Appendix A 3 for details).

We analyze various quantities to estimate the RG dimensions Y_l : the original quantities C_l and D_l introduced in Sec. II B, their counterpart \bar{C}_l and \bar{D}_l computed at the

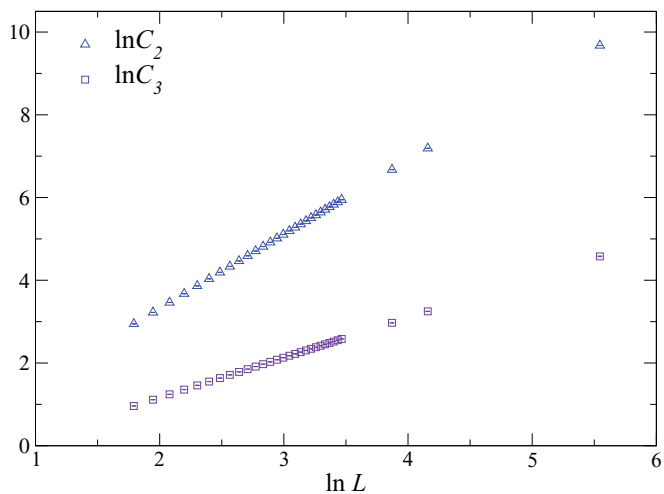


FIG. 1. (Color online) Log-log plots of C_2 and C_3 vs L at β_c for the $O(3)$ ϕ^4 model at $\lambda = 4.5$. The errors of the data are hardly visible.

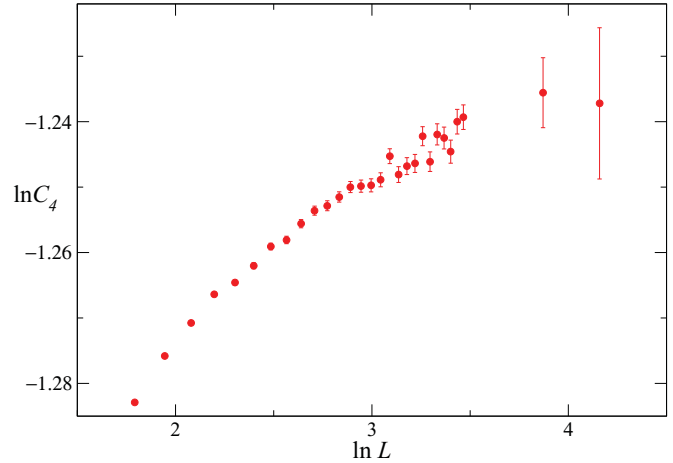


FIG. 2. (Color online) Log-log plots of C_4 vs L at β_c for the $O(3)$ ϕ^4 model at $\lambda = 4.5$.

fixed value $\xi/L = 0.5644$ (which is a good estimate of the large-volume limit of ξ/L at β_c , see Appendix B), and also the quantities $C_{l,\text{imp}} = \bar{U}_4^x \bar{C}_l$ and $D_{l,\text{imp}} = \bar{U}_4^x \bar{D}_l$ again taken at $\xi/L = 0.5644$ where the exponent x is chosen to further suppress the leading corrections (see Refs. 3 and 32 for details). In principle, the latter quantities should be more suitable for the numerical analysis. Indeed, by fixing $\xi/L = 0.5644$ we avoid the error due to the uncertainty of β_c , and by the construction of the improved observables the effect of the uncertainty of λ^* is strongly reduced. However also subleading corrections vary, and, unfortunately, they become numerically larger in these cases. Nevertheless it is useful to study these quantities. Since the amplitudes of corrections change, these modified quantities give us additional control over the systematic error that is caused by truncated ansatz.

Let us now discuss the analysis of the quantities D_l in some detail. In the case of the quantities C_l we proceed in a similar way. Following the discussion of Sec. III A 1 we first analyze the ratios

$$r_{D_l} = \frac{D_l(\lambda = 5, \beta = 0.687564)}{D_l(\lambda = 4, \beta = 0.68439)}, \quad (33)$$

where $\beta = 0.687564$ and $\beta = 0.68439$ are the estimates for β_c given in Table V of Ref. 6 and

$$r_{\bar{D}_l} = \frac{\bar{D}_l(\lambda = 5)}{\bar{D}_l(\lambda = 4)}. \quad (34)$$

We fit these ratios to the ansatz

$$r = c(1 + bL^{-\omega}), \quad (35)$$

where we set $\omega = 0.79$. To give an idea how accurately the coefficient b can be determined, let us discuss a few examples. In the case of D_2 a fit of all data with $L \geq L_{\text{min}}$ with $L_{\text{min}} = 6$ gives the result $b = -0.00841(38)$ and $\chi^2/\text{DOF} = 3.80/9$. Increasing L_{min} the estimate of b changes very little, for example, for $L_{\text{min}} = 8$ we obtain $b = -0.00830(64)$ and $\chi^2/\text{DOF} = 3.58/7$. In the following analysis we shall assume $b = -0.0083(7)$. In the case of \bar{D}_2 we obtain for $L_{\text{min}} = 7$ the result $b = 0.00348(24)$ and $\chi^2/\text{DOF} = 8.48/8$ and for $L_{\text{min}} = 9$ the results $b = 0.00407(41)$ and $\chi^2/\text{DOF} = 2.34/6$. In the following analysis we shall assume $b = 0.004(1)$. It

is interesting to observe that by taking D_2 at $\xi/L = 0.5644$ instead of β_c even the sign of the correction amplitude changes. For D_4 we obtain $b = 0.0313(45)$ and $\chi^2/\text{DOF} = 7.49/8$ using $L_{\min} = 7$. The result changes little when we increase L_{\min} . For example, we get $b = 0.0303(93)$ and $\chi^2/\text{DOF} = 7.42/6$ for $L_{\min} = 9$. In the following we shall assume $b = 0.03(1)$. For \bar{D}_4 we get instead $b = 0.05(1)$. Note that also the correction amplitudes of D_4 and \bar{D}_4 are different.

In order to compute the quantities \mathcal{I}_{D_l} and $\mathcal{I}_{\bar{D}_l}$, defined as in Eq. (29) to suppress the residual leading scaling corrections, we use $b_U(5,4) = -0.01126(4)$ and $a_U(4,5) = 0.007(4)$ as obtained in Appendix B 2. In the product $\bar{U}_4^x \bar{D}_l$ the choice $x = -\bar{U}_4^* b/b_U$ eliminates leading corrections to scaling. The advantage of this quantity is that it does not require a_U , which is affected by a relatively large error.

Next we have fitted the resulting quantities with the ansaetze

$$\mathcal{I}_{D_l}(\lambda_0; L) \equiv D_l(\lambda_0; L) \left[1 - \frac{b_l(\lambda_1, \lambda_2)}{b_U(\lambda_1, \lambda_2)} a_U(\lambda_0) L^{-\omega} \right] = a L^{Y_l} \quad (36)$$

and

$$\mathcal{I}_{\bar{D}_l} = a L^{Y_l} (1 + d L^{-1.6}) \quad (37)$$

and correspondingly for the quantities $\mathcal{I}_{\bar{D}_l}$ and $\bar{U}_4^x \bar{D}_l$. The effect of the uncertainties of β_c , and the quantities a_U , b_U , b_l need to construct \mathcal{I}_{D_l} , $\mathcal{I}_{\bar{D}_l}$, and $\bar{U}_4^x \bar{D}_l$, are estimated by varying these input parameters. For example, in order to estimate the uncertainty of $\mathcal{I}_{\bar{D}_l}$ induced by the uncertainty of a_U , we have repeated the fits using data where we have used in Eq. (29) the central value of a_U plus its error instead of the central value.

In Table III we report results of fits for \mathcal{I}_{D_2} , $\mathcal{I}_{\bar{D}_2}$, and $\bar{U}_4^x \bar{D}_2$. We note that the estimates of Y_2 obtained by the two fits and the three quantities differ by larger amounts than their statistical errors. Hence systematic errors are more important than the statistical one. Taking into account also the results obtained for C_4 and the quantities derived from it we arrive at our final estimate $Y_2 = 1.7906(3)$ which covers most of the acceptable fits and also takes into account the uncertainties in the construction of \mathcal{I}_{D_2} , $\mathcal{I}_{\bar{D}_2}$, and $\bar{U}_4^x \bar{D}_2$. In a similar way we arrive at the estimate $Y_3 = 0.9616(10)$ of the spin-3 RG dimension.

Finally, let us discuss the analysis leading to our estimate of Y_4 . In Table IV we give some results of the fits with the ansaetze (36) and (37). As our final result we quote $Y_4 = 0.013(4)$ which covers all estimates given in Table IV. The uncertainties in the construction of \mathcal{I}_{D_4} , $\mathcal{I}_{\bar{D}_4}$, and $\bar{U}_4^x \bar{D}_4$ are taken into account. Furthermore, this estimate is fully consistent with the results obtained from the analysis of \mathcal{I}_{C_4} , $\mathcal{I}_{\bar{C}_4}$, and $\bar{U}_4^x \bar{C}_4$.

TABLE III. Fits of \mathcal{I}_{D_2} (columns 2 and 3), $\mathcal{I}_{\bar{D}_2}$ (columns 4 and 5), and $\bar{U}_4^x \bar{D}_2$ (columns 6 and 7) with the ansaetze (36) and (37). We give the L_{\min} of the fit, which is typically the smallest L_{\min} that produces an acceptable fit and the result for Y_2 .

Ansatz	L_{\min}	Y_2	L_{\min}	Y_2	L_{\min}	Y_2
(36)	24	1.79067(5)	28	1.79078(3)	32	1.79080(5)
(37)	12	1.79019(7)	8	1.79053(2)	8	1.79049(2)

TABLE IV. Fits of \mathcal{I}_{D_4} (columns 2 and 3), $\mathcal{I}_{\bar{D}_4}$ (columns 4 and 5), and $\bar{U}_4^x \bar{D}_4$ (columns 6 and 7) with the ansaetze (36) and (37). We give the L_{\min} of the fit, which is typically the smallest L_{\min} that produces an acceptable fit and the result for Y_4 .

Ansatz	L_{\min}	Y_4	L_{\min}	Y_4	L_{\min}	Y_4
(36)	14	0.0143(8)	14	0.0142(8)	16	0.0160(10)
(37)	12	0.0122(26)	12	0.0127(25)	12	0.0122(26)

We conclude with a few remarks on the possibility of further improving the estimate of Y_4 . Its accuracy is essentially limited by the fact that the variances of the correlators C_4 and D_4 rapidly increase with increasing lattice size, not allowing us to get accurate results for large lattices, indeed extremely high statistics are necessary for $L \gtrsim 32$ already. Thus, the reduction of the systematic error due to the truncation of the Wegner expansion appears quite problematic because it can only get reduced by accurate results for larger lattice sizes. One purely technical way in this direction could be the simulation with local algorithms (Metropolis + many overrelaxation sweeps) on GPUs (graphics cards).

2. The $O(2)$ and $O(4)$ models

In the cases of the XY and $O(4)$ universality classes we have determined the exponents along similar lines, obtaining the results reported in Table II. We only mention that, since in the case of the XY universality class, λ^* and β_c at $\lambda = 2.1$ are accurately known,³ we abstained from analyzing the quantities $\bar{U}_4^x \bar{C}_l$ and $\bar{U}_4^x \bar{D}_l$. In the case of the $O(4)$ universality class the situation is different; here we do not have a very precise estimate of λ^* and also β_c is only moderately well known at $\lambda = 12.5$, where most of our simulations are performed. Therefore we have based our analysis on \bar{C}_l and \bar{D}_l and the improved quantities $\bar{U}_4^x \bar{C}_l$ and $\bar{U}_4^x \bar{D}_l$, where the quantities are taken at $\xi/L = 0.547$.

IV. CONCLUSIONS AND DISCUSSION OF SOME APPLICATIONS

In this paper we study the effects of anisotropic perturbations in three-dimensional $O(N)$ -symmetric vector models, which cannot be related to an external vector field coupled to the order parameter, but are represented by composite operators with more complex transformation properties under the $O(N)$ group. For the models with $N = 2, 3, 4$, we determine the RG dimensions Y_l of the anisotropic perturbations associated with the first few spin values of the representations of the $O(N)$ group because the lowest spin values give rise to the most important effects. This is the first numerical study based on MC simulations for the spin-2 and spin-3 perturbations, while MC results for spin-4 operators were already reported in Ref. 24.

We present FSS analyses of MC simulations of improved Hamiltonians with suppressed leading corrections to scaling, which allows us to achieve a robust control of the systematic errors arising from scaling corrections. Our results are reported in Table II, together with earlier results by various approaches. They are in good agreement with the estimates obtained by

field-theoretical methods, by resumming high-order perturbative series. Our results show that spin-4 perturbations in three-dimensional Heisenberg systems are relevant, with a quite small RG dimension $Y_4 = 0.013(4)$, which may give rise to very slow crossover effects in systems with small spin-4 anisotropy.

In the following we discuss a number of physical systems where the results of this paper for the anisotropic perturbations can be used to infer the critical behavior of some physically interesting quantities.

A. Critical exponents of secondary order parameters

Beside the standard critical exponents associated with the order parameter, density wave XY systems allow to measure the higher-harmonic critical exponents related to secondary order parameters, which can be theoretically represented by polynomials of the order parameter with spin representation higher than one, such as the spin- l operators $Q_l(\phi_x)$ [cf. Eqs. (5)–(7)].

The behavior at zero-momentum of the correlation functions involving the operators $Q_l(\phi_x)$ can be described by introducing an appropriate external field h_l coupled with $Q_l(\phi_x)$, and writing the singular part of the free energy as in Eq. (1). Then, differentiating with respect to h_l , we obtain the behavior of the secondary magnetizations in the broken phase,

$$\langle Q_l(\phi_x) \rangle \sim |t|^{\beta_l}, \quad \beta_l = \nu(d - Y_l). \quad (38)$$

Our estimates of the RG dimensions Y_l for the XY universality class $Y_2 = 1.7639(11)$, $Y_3 = 0.8915(20)$, and $Y_4 = -0.108(6)$ give

$$\beta_2 = 0.8303(8), \quad \beta_3 = 1.4163(13), \quad \beta_4 = 2.09(4). \quad (39)$$

Moreover, the nonanalytic scaling behaviors of spin- l susceptibilities are

$$\chi_l \equiv \sum_x \langle Q_l(\phi_0) Q_l(\phi_x) \rangle \sim |t|^{-\gamma_l}, \quad \gamma_l = \nu(2Y_l - d), \quad (40)$$

with

$$\gamma_2 = 0.3545(15), \quad \gamma_3 = -0.817(3), \quad \gamma_4 = -2.160(8). \quad (41)$$

Note that the power law $|t|^{-\gamma_l}$ in the susceptibility χ_l represents the leading term only if $\gamma_l > 0$, otherwise the nonuniversal analytic contributions provide the dominant behavior (see, e.g., Ref. 33). We also mention that the structure factor, obtained by Fourier transforming the correlation function $G_l(x - y) = \langle Q_l(\phi_x) Q_l(\phi_y) \rangle$, is expected to behave as $\tilde{G}_l(q) \sim |t|^{-\gamma_l} f_l(q\xi)$, where f_l is a universal function (see Ref. 33 and references therein).

Discussions of the experimental systems and results for the higher-harmonic exponents can be found in Refs. 2, 25, and 33. The experimental estimates are in substantial agreement with the theoretical results. Here we only mention a few of them. Analyses^{15,16,34} of the experimental data near the smectic-C-tilted-hexatic-I transition provided estimates of the crossover exponent $\phi_l = Y_l\nu$. By replacing $\nu = 0.6717$, they give

$Y_2 = 1.7(1)$ and $Y_3 = 0.6(3)$. In Ref. 20 the estimates $\beta_2 = 0.87(1)$ and $\beta_3 = 1.50(4)$ were obtained for Rb_2ZnCl_4 .

B. Magnets with cubic symmetry

The magnetic interactions in crystalline solids with cubic symmetry, like iron or nickel, are usually modeled by using the O(3)-symmetric Heisenberg Hamiltonian with short-range spin interactions, such as

$$H_{\text{spin}} = -J \sum_{\langle ij \rangle} S_i \cdot S_j, \quad (42)$$

where $S^2 = 1$ and the sum is over nearest neighbors. However, this is a simplified model, since other interactions are present. Among them, the magnetic anisotropy that is induced by the lattice structure (the so-called crystal field) is particularly relevant experimentally (see, e.g., Ref. 35). In cubic-symmetric lattices it gives rise to additional single-ion contributions, the simplest one being

$$\sum_i \sum_a S_i^{a4}. \quad (43)$$

These terms are usually not considered when the critical behavior of cubic magnets is discussed. However, this is strictly justified only if these nonrotationally invariant interactions, that have the reduced symmetry of the lattice, are irrelevant in the RG sense. The corresponding cubic-symmetric perturbation $\sum_a \Phi^{a4}$ to the O(N) theory is a particular combination of spin-4 operators $P_{4,4}^{abcd}$ and of the spin-0 term $P_{4,0}$,

$$\sum_a \Phi^{a4} = \sum_{a=1}^N P_{4,4}^{aaaa}(\Phi) + \frac{3}{N+2} P_{4,0}(\Phi). \quad (44)$$

Since $P_{4,0}$ is always irrelevant, the relevance of the cubic-symmetric anisotropy is related to the value of the spin-4 RG dimension Y_4 , and in particular to its sign. Our results, and in particular $Y_4 = 0.013(4)$ for the O(3) universality class, show that the cubic perturbation is relevant at the three-dimensional O(N) fixed point when $N \geq 3$, confirming earlier FT results.^{26,36–38} This implies that for $N \geq 3$ the asymptotic critical behavior is described by another cubic-symmetric fixed point, see, for example, Ref. 2 for a general discussion of the RG flow in the Φ^4 theories with cubic-symmetric anisotropy. However, differences between the Heisenberg and cubic critical exponents are very small,¹¹ for example ν differs by less than 0.1%, which is much smaller than the typical experimental error for Heisenberg systems.² Therefore, distinguishing the cubic and the Heisenberg universality class is very hard in experiments.

C. Multicritical phenomena in O(n_1) \oplus O(n_2)-symmetric systems

The competition of distinct types of ordering gives rise to multicritical behaviors. The multicritical behavior arising from the competition of two types of ordering characterized by O(n) symmetries is determined by the RG flow of the most general O(n_1) \oplus O(n_2)-symmetric LGW Hamiltonian involving two

fields ϕ_1 and ϕ_2 with n_1 and n_2 components respectively, that is,¹³

$$\mathcal{H}_{\text{mc}} = \int d^d x \left[\frac{1}{2}(\partial_\mu \phi_1)^2 + \frac{1}{2}(\partial_\mu \phi_2)^2 + \frac{1}{2}r_1 \phi_1^2 + \frac{1}{2}r_2 \phi_2^2 + u_1(\phi_1^2)^2 + u_2(\phi_2^2)^2 + w\phi_1^2\phi_2^2 \right]. \quad (45)$$

A multicritical point (MCP) is achieved when r_1 and r_2 are tuned to their critical value, and the corresponding multicritical behavior is determined by the stable FP of the RG flow of the quartic parameters. It may occur at the intersection of two critical lines characterized by different $O(n_1)$ and $O(n_2)$ order parameters.

An interesting possibility is that the stable FP has $O(n_1 + n_2)$ symmetry, so that the symmetry gets effectively enlarged approaching the MCP. The stability properties of the $O(n_1 + n_2)$ symmetric FP can be inferred by noting¹¹ that the Hamiltonian (45) contains combinations of spin-2 and spin-4 polynomial operators with respect to the $O(n_1 + n_2)$ group, which are invariant under the symmetry $O(n_1) \oplus O(n_2)$. Defining Φ as the $(n_1 + n_2)$ -component field (ϕ_1, ϕ_2) , they are given by the spin-0 operators Φ^2 and $(\Phi^2)^2$, by the spin-2 operators

$$O_{2,2} = \sum_{a=1}^{n_1} P_{2,2}^{aa} = \phi_1^2 - \frac{n_1}{n_1 + n_2} \Phi^2, \quad O_{4,2} = \Phi^2 O_{2,2}, \quad (46)$$

and by the spin-4 operator

$$O_{4,4} = \sum_{a=1}^{n_1} \sum_{b=n_1+1}^{n_2} P_{4,4}^{aabb} = \phi_1^2 \phi_2^2 - \frac{\Phi^2(n_1 \phi_2^2 + n_2 \phi_1^2)}{n_1 + n_2 + 4} + \frac{n_1 n_2 (\Phi^2)^2}{(n_1 + n_2 + 2)(n_1 + n_2 + 4)}. \quad (47)$$

The $O(n_1 + n_2)$ FP controls the multicritical behavior if it is stable against the fourth-order perturbations, and, in particular, the dominating spin-4 perturbation $O_{4,4}$ (the perturbation $O_{4,2}$ is expected to be irrelevant after the subtraction of its lower-dimension spin-2 content¹¹).

Our FSS MC results for the spin-4 RG dimensions Y_4 (see Table II), and, in particular, that for the $O(3)$ universality class, provide a conclusive evidence that $Y_4 > 0$ for $n_1 + n_2 \geq 3$, confirming earlier indications from FT computations.¹¹ Therefore the enlargement of the symmetry $O(n_1) \oplus O(n_2)$ to $O(n_1 + n_2)$ does not occur unless an additional parameter is tuned beside those associated with the quadratic perturbations. We may only observe an enlargement of the symmetry to $O(2)$ when two Ising lines meet. In this case the RG dimension Y_2 of the spin-2 operator $O_{2,2}$ provides the crossover exponent $\phi = \nu Y_2 = 1.1848(8)$ at the MCP.

These results can be applied to the study of the phase diagram of anisotropic antiferromagnets in a uniform magnetic field H_\parallel parallel to the anisotropy axis, which present a MCP in the $T - H_\parallel$ phase diagram, where two critical lines belonging to the XY and Ising universality classes meet.^{13,14} Experimental realizations of these systems are reported in Refs. 39–41, which typically show phase diagrams with a bicritical MCP. The initial hypothesis of an enlarged $O(3)$

symmetry at the MCP, on the basis of low-order FT calculations,¹⁴ was then questioned by high-order FT computations¹¹ (see also Ref. 42), indicating a very weak instability of the $O(3)$ FP. This instability was then questioned by the numerical MC study of Ref. 43, where evidence of a $O(3)$ -symmetric bicritical point is claimed in the phase diagram of the so-called XXZ model, which models anisotropic antiferromagnets in an external field, showing a MCP where an XY and an Ising transition line meet. Actually, this result was one of the major motivations of this numerical work to further check the relevance of the spin-4 perturbation at the $O(3)$ FP, because an asymptotic $O(3)$ multicritical behavior requires $Y_4 < 0$. Our MC results fully confirm earlier high-order FT results, that is, the relevance of the spin-4 $O(3)$ -breaking term which are generally present in these models. This implies that a bicritical point in the Heisenberg universality class is excluded, unless one achieves a complete cancellation of the spin-4 term by an appropriate fine tuning.

As inferred by FT calculations, the actual stable FP has a biconical structure.¹¹ A quantitative analysis of the biconical FP shows that its critical exponents are very close to the Heisenberg ones. For instance, the correlation-length exponent ν differs by less than 0.001 in the two cases. Thus, it should be very hard to distinguish the biconical from the $O(3)$ critical behavior in experiments or numerical works based on Monte Carlo simulations.

The crossover exponent describing the crossover from the unstable $O(3)$ critical behavior is very small, that is, $\phi_4 = \nu Y_4 = 0.009(3)$, so that systems with a small effective breaking of the $O(3)$ symmetry show a very slow crossover toward the biconical critical behavior or, if the system is outside the attraction domain of the biconical FP, toward a first-order transition. Thus, they may show the eventual asymptotic behavior only for very small values of the reduced temperature. Likely, the numerical analysis of Ref. 43 was just observing crossover effects.

ACKNOWLEDGEMENT

This work was supported by the DFG under Grant No. HA 3150/2-2.

APPENDIX A: MONTE CARLO SIMULATIONS

1. Monte Carlo algorithm

For our Monte Carlo simulations we have used a hybrid of the local Metropolis, the local overrelaxation and the single cluster⁴⁴ algorithm. The proposals for the local Metropolis update are given by

$$\phi'_x = \phi_x + s r_x, \quad (A1)$$

where s controls the step size and the components of the random vector r_x are uniformly distributed in the interval $[-0.5, 0.5]$. This proposal is accepted with the standard acceptance probability

$$P_{\text{acc}} = \min[1, \exp(-\Delta\mathcal{H})]. \quad (A2)$$

The step size s is chosen such that the acceptance rate is roughly 50%. In the case of the local overrelaxation update, the new value of the field is given by

$$\phi'_x = 2 \frac{\phi_x \cdot \Phi_x}{(\Phi_x)^2} \Phi_x - \phi_x, \quad (\text{A3})$$

where $\Phi_x = \sum_{y,m,x} \phi_y$ is the sum over all fields that live on sites y that are nearest neighbors of x . In the case of the local updates we run through the lattice in typewriter fashion. Going through the lattice once is called one sweep. We use the following cycle of updates: One Metropolis sweep, one overrelaxation sweep, $L/2$ single cluster updates, two overrelaxation sweeps, and finally $L/2$ single cluster updates. In this cycle we compute the observables after $L/2$ single cluster updates, that is, twice.

The average size of a cluster is proportional to the magnetic susceptibility that grows like $L^{2-\eta}$. Therefore, with our choice of $L/2$ single cluster updates per cycle, the fraction of sites that is updated by the cluster algorithm in one cycle of the algorithm stays roughly constant. We also note that the overrelaxation update takes very little CPU time compared with the Metropolis update. For $L = 32$ and $N = 3$ the CPU time needed for one overrelaxation sweep, one Metropolis sweep, and $L/2$ single cluster updates roughly behave as 1 : 4 : 3.

In all our simulations we have used the SIMD-oriented fast Mersenne twister algorithm⁴⁵ as pseudo-random number generator.

2. Statistics of the simulation

In the case of the XY universality class, we performed most of our simulations at $\lambda = 2.1$ and $\beta = 0.5091503$. We simulated the lattice sizes $L = 6, 7, 8, \dots, 18$ and 20, 22, 24, 26, 28. Throughout we performed 10^9 measurements. In total these simulations took about 7 months of CPU time on a single core of a Quad-Core AMD Opteron Processor 2378 running at 2.4 GHz. In addition we performed simulations at $\lambda = 2.2$ and $\beta = 0.508336$ where we simulated the lattice sizes $L = 6, 7, 8, \dots, 12$. The results for $\lambda = 2.2$ are used to estimate the effect of the uncertainty of λ^* . Note that $\lambda^* = 2.15(5)$.³ The values of β chosen for the simulations at $\lambda = 2.1$ and 2.2 are the estimates of β_c given in Table II of Ref. 3.

In the O(3) case we performed most simulations for $\lambda = 4.5$ which is close to our old estimate $\lambda^* = 4.6(4)$.⁶ We simulated at $\beta = 0.686238$ which is close to the estimate $\beta_c = 0.6862385(20)$.⁶ For the lattice sizes $L = 6, 7, 8, 9, \dots, 16$ we performed 10^9 measurements, for $L = 17, 18, \dots, 32$ between 1.1×10^9 and 1.2×10^9 measurements and 5×10^8 , 2.5×10^8 , and 10^6 measurements for $L = 48, 64$, and 256, respectively. In total these simulations took about 4 years of CPU time on a single core of a Quad-Core AMD Opteron Processor 2378 running at 2.4 GHz. In addition, we performed MC simulations at $\lambda = 4.0$, $\beta = 0.68439$ and $\lambda = 5.0$, $\beta = 0.687564$ on lattices of the size $L = 6, 7, 8, \dots, 16$. Throughout we performed 10^9 measurements. These results are used to determine our new estimate of λ^* and the effect of the uncertainty of λ^* on our estimates of the RG exponents.

In the O(4) case most of our simulations were done for $\lambda = 12.5$ and $\beta = 0.9095167$. For $L = 6, 7, 8, \dots, 18$ and 20, 22, 24, 26, 28 we performed 10^9 measurements and for $L = 40$ we performed 6.5×10^8 measurements. For $L = 256$ we performed 10^6 measurements and simulated at $\beta = 0.909513$, which was our preliminary value of β_c . This simulation was done to get a better estimate of β_c . In this simulation we did not measure the quantities C_l and D_l . The estimate $\beta = 0.9095167$ used above was obtained by requiring that $\xi/L = 0.547$ which is the result for the large volume limit $(\xi/L)^*$ of Ref. 8. In addition, in order to determine λ^* and the effect of the uncertainty of λ^* on the accuracy of our estimates of the RG exponents, we have simulated at $\lambda = 14$ the lattice sizes $L = 6, 7, 8, \dots, 12$; $\lambda = 18$ the lattice sizes $L = 6, 7, 8, \dots, 12$; $\lambda = 22$ the lattice sizes $L = 6, 7, 8, \dots, 16, 18, 20$; $\lambda = 30$ and 32 the lattice size $L = 6$; and for $\lambda = \infty$ the lattice sizes $L = 6, 7, 8, \dots, 12, 16, 24, 32$. Throughout the statistics is 10^9 measurements.

Our MC simulations were essentially designed to achieve accurate results for the spin-4 RG dimension Y_4 , whose estimate is much harder than Y_2 and Y_3 , and it is essentially obtained from the high-statistics data for $L \gtrsim 30$ (see the discussion of Appendix A 3). In the case of the O(3) and O(4) models the simulations for larger lattices, beside contributing to make the estimates of Y_2 and Y_3 more accurate, allows us to improve the estimates of the critical parameters β_c and λ^* (as explained in Appendix B). We did not perform MC simulations for $L > 28$ in the case of the O(2) ϕ^4 model because the estimates of β_c and λ^* reported in Ref. 3 were already satisfactory.

The CPU time used for the whole study amounts to roughly 7 years on a single core of a Quad-Core AMD Opteron Processor 2378 running at 2.4 GHz.

3. Variance of the observables

The behavior of the variance of the quantities considered in our MC simulations strongly affects the design of our study. The main problem, as already observed in Ref. 24 is that the relative statistical error, at a fixed number of updates, of C_4 and D_4 rapidly increases with the lattice size. Therefore we have to focus on smaller lattice sizes than one would do in a study mainly aiming at the exponents ν and η .

Let us discuss this problem in a bit more detail at the example of the simulations for $N = 3$, $\lambda = 4.5$, and the quantities D_l . Since we average over 10 000 measurements at simulation time, we cannot disentangle integrated autocorrelation time and variance of the quantities. Therefore in the following we discuss the relative statistical error, normalized to 10^9 measurements. In the case of D_4 this relative statistical error is increasing from 0.000175 for $L = 6$ up to 0.051 for $L = 256$. This increase is well described by a power law $e \propto L^x$, with $x \approx 1.45$. Also in the case of D_3 the relative error is increasing; 0.000064 for $L = 6$ up to 0.00022 for $L = 256$. However here the increase is smaller; it is characterized by the exponent $x \approx 0.3$. Interestingly, for D_2 we find that the relative statistical error is even decreasing a bit; 0.000037 for $L = 6$ down to 0.00003 for $L = 256$. The corresponding exponent is $x \approx -0.05$. This behavior can be compared with that of the relative error of the slope of the Binder cumulant or the

second moment correlation length. These quantities are used to determine the critical exponent ν . In both cases we find a mild increase of the relative error, which is characterized by the exponents $x \approx 0.06$ and $x \approx 0.14$, respectively.

As shown in Ref. 24, the problem of the large variance of C_4 can be reduced by performing a larger number of overrelaxation updates which are relatively cheap in terms of CPU time and measure C_4 after each such update. This way one could improve the efficiency in terms of $1/[(\text{CPU time}) \times \text{error}^2]$ of C_4 or D_4 by about a factor of 2 compared with the update cycle used in our simulations. However, since this would have an adverse effect with respect to all other quantities that we have measured we abstained from this.

For several observables, such as the susceptibility and the quartic Binder cumulant, the statistical errors at fixed ξ/L are smaller than those at fixed β close to β_c . Some comparisons are reported in Refs. 3 and 46. This is due to cross correlations and to a reduction of the effective autocorrelation times. Taking C_l or D_l at ξ/L fixed reduces the variance in a l -dependent way. For the C_4 and D_4 cases there is virtually no reduction of the error. For $L = 6$ there is still an improvement by a few percent, however with increasing L the ratio of errors goes rapidly to 1. In the $l = 3$ case we observe a mild improvement by fixing ξ/L . For C_3 the ratio of statistical errors is 1.9 for $L = 6$, 1.10 for $L = 64$, and 1.017 for $L = 256$. In the case of D_3 , the ratio of statistical errors is 1.33 for $L = 6$, 1.06 for $L = 64$, and 1.014 for $L = 256$. The reduction of the statistical error is most significant in the $l = 2$ case. For C_2 the ratio of the statistical errors is 3.49 for $L = 6$, it decreases to 2.65 at $L = 27$, and then increases again; 2.69 at $L = 64$ and 2.88 for $L = 256$. For D_2 the ratio of the statistical errors is 2.21 for $L = 6$, has its minimum 1.91 at $L = 23$, takes 2.02 for $L = 64$ and 2.20 for $L = 256$.

APPENDIX B: SOME FURTHER RESULTS FOR THE $O(N)$ VECTOR MODELS, $N = 3$ AND 4

1. New estimate for β_c

In order to determine β_c of the $O(3)$ ϕ^4 model at $\lambda = 4.5$, we fit the data for ξ/L and U_4 to the ansatz

$$R(L, \beta_c) = R^*, \quad (\text{B1})$$

$$R(L, \beta_c) = R^* + aL^{-0.79}, \quad (\text{B2})$$

and

$$R(L, \beta_c) = R^* + aL^{-0.79} + bL^{-\epsilon}, \quad (\text{B3})$$

where either $\epsilon = 1.6$ or $\epsilon = 2$. Here we take 0.79 as value of the correction exponent ω . By replacing it with 0.77 say, our results for β_c and R^* change only very little. In this study, we only calculate first derivatives of the quantities; therefore in the fits we use the approximation

$$R(L, \beta) \approx R(L, \beta_s) + a(\beta - \beta_s), \quad (\text{B4})$$

where β_s is the value of the inverse temperature used for the simulation. Since β_s is very close to our final result for β_c , the error due to the truncation of the Taylor-series can be ignored.

Let us first discuss the analysis of ξ/L . Taking no corrections into account, that is, fitting with the ansatz (B1), χ^2/DOF remains unacceptably large until most of our lattice

sizes are discarded. Including $L = 48, 64$, and 256, we obtain $(\xi/L)^* = 0.56421(5)$, $\beta_c - \beta_s = -0.0000006(5)$, and $\chi^2/\text{DOF} = 1.72/1$. Using the ansatz (B2), that is, adding a correction term $aL^{-0.79}$, we get a χ^2/DOF smaller than 1 starting from $L_{\min} = 12$, where all lattice sizes $L \geq L_{\min}$ are taken into account. Discarding further data points χ^2/DOF is further decreasing and $(\xi/L)^*$ and $\beta_c - \beta_s$ move monotonically. For $L_{\min} = 18$ we find $(\xi/L)^* = 0.56405(5)$ and $\beta_c - \beta_s = -0.00000067(38)$. Adding a further correction, we get acceptable values of χ^2/DOF already for $L_{\min} = 7$. But also here χ^2/DOF still further decreases and $(\xi_{2\text{nd}}/L)^*$ and $\beta_c - \beta_s$ move monotonically with increasing L_{\min} . For $\epsilon = 1.6$ we obtain the results $(\xi_{2\text{nd}}/L)^* = 0.56386(10)$ and $\beta_c - \beta_s = -0.00000119(48)$ for $L_{\min} = 12$. For $\epsilon = 2$ and $L_{\min} = 12$, we get the results $(\xi_{2\text{nd}}/L)^* = 0.56391(8)$ and $\beta_c - \beta_s = -0.0000011(46)$. For the Binder cumulant similar results can be found. We arrive at the final results $\beta_c(\lambda = 4.5) = 0.6862368(10)$ and

$$(\xi/L)^* = 0.5639(2), \quad U_4^* = 1.1394(3). \quad (\text{B5})$$

The error bars are chosen such that the results of the different fits are covered.

A similar analysis for the $O(4)$ symmetric ϕ^4 model at $\lambda = 12.5$ leads to estimates $U_4^* = 1.0942(3)$, $\xi/L = 0.5471(3)$, and $\beta_c = 0.909517(2)$.

2. Determination of λ^*

Next we determine the value of λ^* where leading corrections to scaling vanish. To this end we study

$$\bar{U}_4(L) = U_4(L, \beta_f), \quad (\text{B6})$$

where β_f is determined by the equation

$$\frac{\xi(L, \beta_f)}{L} = 0.5644, \quad (\text{B7})$$

where 0.5644 is the result for $(\xi/L)^*$ of Ref. 6. In order to compute \bar{U}_4 we use the first order Taylor expansion (B4) of ξ/L and U_4 around the simulation point β_s . For $L = 12$, $\lambda = 4.5$ we simulate at a number of different β_s , to check whether this approximation is sufficient for our purpose. In particular we find that for $\lambda = 4.5$ the difference between $\beta_s = 0.686238$ and β_f is sufficiently small that contributions $\propto (\beta - \beta_s)^2$ can be ignored. Due to scaling, we expect that this also holds for all of the lattice sizes that we have simulated.

First we fit our data obtained at $\lambda = 4.5$ with a number of different ansatz

$$\bar{U}_4 = \bar{U}_4^* + aL^{-0.79}, \quad (\text{B8})$$

$$\bar{U}_4 = \bar{U}_4^* + aL^{-0.79} + bL^{-\epsilon_1}, \quad (\text{B9})$$

and

$$\bar{U}_4 = \bar{U}_4^* + aL^{-0.79} + bL^{-\epsilon_1} + cL^{-\epsilon_2}. \quad (\text{B10})$$

Also here we fix $\omega = 0.79$; the final results change only little when we replace it with $\omega = 0.77$. In the case of the ansatz (B9) we set $\epsilon_1 = 1.6$ or 2. Finally in ansatz (B10) we add two terms with subleading corrections. We have fitted using various choices for ϵ_1 and ϵ_2 .

In our fits we take into account all lattices sizes $L \geq L_{\min}$. In the case of the ansatz (B8) we get an acceptable χ^2/DOF

starting from $L_{\min} = 22$. From this fit we get $a = 0.00254(31)$. Further increasing L_{\min} , a is monotonically increasing; for $L_{\min} = 30$ we obtain $a = 0.0037(6)$.

Fitting with the ansatz (B9) and $\epsilon_1 = 1.6$ we obtain an acceptable χ^2/DOF already starting from $L_{\min} = 6$. We get $a = 0.01038(27)$ for the correction amplitude. Increasing L_{\min} the correction amplitude remains stable. Using instead $\epsilon_1 = 2$ we get an acceptable χ^2/DOF starting from $L_{\min} = 7$. The corresponding result for the correction amplitude is $a = 0.00586(20)$. Increasing L_{\min} , the value of a increases up to $a = 0.00676(33)$ for $L_{\min} = 10$. For $L_{\min} = 11$ and 12 we get a very similar result. For $L_{\min} = 12$, $\chi^2/\text{DOF} = 14.50/21$ and $15.78/21$ for $\epsilon = 2$ and 1.6 , respectively.

Finally we fit with the ansatz (B9) using $(\epsilon_1, \epsilon_2) = (1.6, 2)$, $(1.6, 1.96)$, or $(1.8, 2)$. The results of such fits are all in the interval $0.005 < a < 0.011$. We conclude $a = 0.007(4)$, where the central value and the error bar are chosen such that the results of the different fits are covered. Next we convert this estimate of the correction amplitude at $\lambda = 4.5$ into a new estimate of λ^* . In order to compute the derivative of a with respect to λ , we study the differences

$$\Delta \bar{U}_4(L) = \bar{U}_4(L, \lambda = 5) - \bar{U}_4(L, \lambda = 4). \quad (\text{B11})$$

In this difference \bar{U}_4^* exactly cancels. Furthermore, subleading corrections should cancel to a large extent. Therefore we fit our data with the ansatz

$$\Delta \bar{U}_4(L) = cL^{-\omega}. \quad (\text{B12})$$

Results of such fits with c and ω as free parameters are given in Table V. Already starting from $L_{\min} = 6$ we get an acceptable χ^2/DOF . Furthermore, the value obtained for ω is fully consistent with the field theoretic estimates $\omega = 0.782(13)$ and $\omega = 0.794(18)$ obtained by the perturbative expansion in three dimensions fixed and the ϵ expansion, respectively.⁴ The facts that χ^2/DOF is small and the result for ω is consistent with the field-theoretical ones already confirms our assumption that for the lattice sizes that we consider, $\Delta \bar{U}_4(L)$ is dominated by the leading correction.

Fitting with $\omega = 0.79$ fixed, to be consistent with the analysis of \bar{U}_4 at $\lambda = 4.5$ above, we find $c = -0.01126(4)$ and $\chi^2/\text{DOF} = 6.0/8$ for $L_{\min} = 8$. The result for c changes little, when L_{\min} is varied. In order to check how well the derivative of a with respect to λ is approximated by the finite difference, we also have fitted $\bar{U}_4(L, \lambda = 5) - \bar{U}_4(L, \lambda = 4.5)$. Here we find $c = -0.00506(4)$ and $\chi^2/\text{DOF} = 5.4/8$ for $L_{\min} = 8$. Also here, the result for c changes little, when L_{\min} is varied.

TABLE V. Fits with the ansatz (B12), O(3) universality class.

L_{\min}	c	ω	χ^2/DOF
6	-0.0109(2)	0.775(9)	6.44/9
7	-0.0109(3)	0.777(12)	6.38/8
8	-0.0111(4)	0.784(16)	5.86/7

TABLE VI. Fits of $\Delta \bar{U}_4(L, 22, 12.5)$ with the ansatz (B12), O(4) universality class.

L_{\min}	c	ω	χ^2/DOF
6	-0.00776(14)	0.777(8)	6.77/11
7	-0.00764(18)	0.771(10)	5.81/10
8	-0.00753(22)	0.765(11)	5.15/9
9	-0.00741(28)	0.759(15)	4.64/8

Using these results we arrive at

$$\lambda^* \approx 4.5 - a(\lambda = 4.5) \left(\frac{\partial a}{\partial \lambda} \right)^{-1} = 4.5 - 0.007(4)/[-2 \times 0.00506(4)] \approx 5.2(4). \quad (\text{B13})$$

We perform a similar analysis in the case of the O(4) universality class. Here β_f is given by

$$\frac{\xi(L, \beta_f)}{L} = 0.547, \quad (\text{B14})$$

where 0.547 is the result for $(\xi/L)^*$ of Ref. 8. First we have analyzed the data for \bar{U}_4 at $\lambda = 12.5$. The analysis is done in much the same way as discussed above in detail for the O(3) universality class. Fixing $\omega = 0.79$ we find $a = 0.007(5)$ as amplitude of the leading correction.

Next we study the difference

$$\Delta \bar{U}_4(L, \lambda_1, \lambda_2) = \bar{U}_4(L, \lambda_1) - \bar{U}_4(L, \lambda_2). \quad (\text{B15})$$

We perform fits for $\lambda_1 = 22$, $\lambda_2 = 12.5$ and $\lambda_1 = \infty$, $\lambda_2 = 12.5$ using the ansatz (B12) with c and ω as free parameters. The results for $\lambda_1 = 22$ and $\lambda_1 = \infty$ are given in Tables VI and VII, respectively.

These results can be compared with $\omega = 0.774(20)$ and $\omega = 0.795(30)$ from the perturbative expansion at three dimensions fixed and the ϵ expansion, respectively.⁴

Fixing $\omega = 0.79$ we obtain $c = -0.00800(2)$ (with $\chi^2/\text{DOF} = 9.77/12$) as amplitude for the differences $\lambda_1 = 22$ and $\lambda_2 = 12.5$ with $L_{\min} = 6$. Taking data only for $L = 6$ we get $c(\lambda_1 = 14, 12.5) = -0.00193(5)$, $c(\lambda_1 = 20, 12.5) = -0.00696(5)$, $c(\lambda_1 = 30, 12.5) = -0.01084(5)$, $c(\lambda_1 = 32, 12.5) = -0.01132(5)$. It is quite clear from these numbers that a linearization of the correction amplitude as a function of λ is not sufficient to compute the estimate of λ^* . For the same reason, we give an asymmetric estimate of the error

$$\lambda^* = 20_{-6}^{+15}. \quad (\text{B16})$$

TABLE VII. Fits of $\Delta \bar{U}_4(L, \infty, 12.5)$ with the ansatz (B12), O(4) universality class.

L_{\min}	c	ω	χ^2/DOF
6	-0.01870(16)	0.787(4)	11.64/7
7	-0.01849(21)	0.783(5)	9.39/6
8	-0.01841(26)	0.781(6)	9.05/5
9	-0.01844(32)	0.782(7)	9.02/4
10	-0.01846(38)	0.782(8)	9.00/3
11	-0.01777(45)	0.769(10)	2.03/2

This value is larger than $\lambda^* = 12.5(4.0)$ that we quote in Ref. 8. However we are quite confident that indeed a λ^* exists for the O(4) case. Note that in the limit $N \rightarrow \infty$ for the simple cubic lattice and the given lattice action, no λ^* exists and that leading corrections are minimal in the limit $\lambda \rightarrow \infty$.¹

3. The magnetic susceptibility and the exponent η

In order to obtain the critical exponent η , we analyze the behavior of

$$\bar{\chi} = \chi(\beta_f), \quad (\text{B17})$$

where in the O(3) case β_f is defined by $\xi(\beta_f)/L = 0.5644$. In the first step of the analysis we eliminate leading corrections to scaling. To this end we analyze the ratios

$$\frac{\bar{\chi}(\lambda = 5)}{\bar{\chi}(\lambda = 4)} = a(1 + cL^{-0.79}), \quad (\text{B18})$$

We obtain a good fit starting from $L_{\min} = 11$. For $L_{\min} = 11$ we obtain $a = 0.99172(8)$, $c = -0.0046(6)$, and $\chi^2/\text{DOF} = 3.11/4$. Therefore in order to eliminate corrections at $\lambda = 4.5$ we follow the strategy discussed in Sec. III A 1. Using $\bar{U}_4 = U_4^* + 0.007(4)L^{-0.79} + \dots$ and $\bar{U}_4(\lambda = 5) - \bar{U}_4(\lambda = 4) = -0.01126(4)L^{-0.79} \dots$ Eq. (29) reads

$$\tilde{\chi} \equiv \bar{\chi}(\lambda = 4.5) \left[1 - \frac{-0.0046(6)}{-0.01126(4)} 0.007(4)L^{-0.79} \right]. \quad (\text{B19})$$

We fit $\tilde{\chi}$ with the ansatz

$$\tilde{\chi} = aL^{2-\eta}, \quad (\text{B20})$$

$$\tilde{\chi} = aL^{2-\eta} + c, \quad (\text{B21})$$

$$\tilde{\chi} = aL^{2-\eta}(1 + bL^{-\epsilon}) + c \quad (\text{B22})$$

with $\epsilon = 1.6$ or $\epsilon = 1.8$. In the case of the ansatz (B20) we obtain very large χ^2/DOF up to $L_{\min} = 32$. For $L_{\min} = 48$ we get $\eta = 0.0375(1)$ and $\chi^2/\text{DOF} = 0.46/1$. Using the ansatz (B21) we get $\chi^2/\text{DOF} \approx 1$ already for $L_{\min} = 16$; for example, for $L_{\min} = 18$ we obtain $\eta = 0.03767(4)$ and $\chi^2/\text{DOF} = 10.11/15$. Using the ansatz (B22) with $\epsilon = 1.6$ we get for $L_{\min} = 10$ the results $\eta = 0.03791(7)$ and $\chi^2/\text{DOF} = 14.55/22$. and for $\epsilon = 1.8$ and $L_{\min} = 8$ we get $\eta = 0.03780(3)$ and $\chi^2/\text{DOF} = 18.74/24$. We redo these fits for $\bar{\chi}$ without correction to check the effect of the uncertainty

of λ^* . We find that the estimates of η change by about 0.0001. Taking into account only fits with ansatz that include the analytic background, we arrive at

$$\eta = 0.0378(3). \quad (\text{B23})$$

In the case of the O(4) universality class, performing a similar analysis we obtain

$$\eta = 0.0360(3). \quad (\text{B24})$$

4. The exponent ν

We estimate the exponent ν from the behavior of the slope of U_4 and ξ/L at β_c :

$$S_R = \left. \frac{\partial R}{\partial \beta} \right|_{\beta=\beta_c} = aL^{1/\nu}(1 + cL^{-\omega} + \dots). \quad (\text{B25})$$

Since we did not plan to compute the exponent ν from the beginning, we did not compute the second derivatives of U_4 and ξ/L with respect to β . Hence we cannot compute the slope at fixed values of U_4 or ξ/L . At $\lambda = 4.5$ we performed MC simulation very close to our final value of β_c . Therefore it is sufficient to have a rather rough estimate of the second derivatives of U_4 and ξ/L in order to compute the first derivatives of U_4 and ξ/L at β_c starting from the first derivatives of U_4 and ξ/L at β_s that we have computed in our simulations. To this end, we simulated for $L = 12$ at a number of different β values. Using these data we compute the second derivatives of U_4 and ξ/L with respect to β by finite differences. The second derivatives are then estimated by $R''(L) = R''(12)(L/12)^{2/\nu}$. Notice that our estimate of $\beta_c = 0.6862368(10)$ is very close to the simulation point $\beta_s = 0.686238$. We analyze the resulting data by fitting with various ansatz that are derived from Eq. (B25). We arrive at $\nu = 0.7118(7)$ from the analysis of the slope of ξ/L and $\nu = 0.7114(11)$ from that of U_4 . The error bars take also into account the uncertainty of λ^* . As our final estimate we quote

$$\nu = 0.7116(10). \quad (\text{B26})$$

By a similar analysis for the O(4) universality class, we obtain

$$\nu = 0.750(2). \quad (\text{B27})$$

*martin.hasenbusch@physik.hu-berlin.de

†ettore.vicari@df.unipi.it

¹J. Zinn-Justin, *Quantum Field Theory and Critical Phenomena*, 3rd ed. (Clarendon, Oxford, 1996).

²A. Pelissetto and E. Vicari, *Phys. Rep.* **368**, 549 (2002).

³M. Campostrini, M. Hasenbusch, A. Pelissetto, and E. Vicari, *Phys. Rev. B* **74**, 144506 (2006).

⁴R. Guida and J. Zinn-Justin, *J. Phys. A* **31**, 8103 (1998).

⁵K. E. Newman and E. K. Riedel, *Phys. Rev. B* **30**, 6615 (1984).

⁶M. Campostrini, M. Hasenbusch, A. Pelissetto, P. Rossi, and E. Vicari, *Phys. Rev. B* **65**, 144520 (2002).

⁷We use the new estimate $\lambda^* = 5.2(4)$ to update the high-temperature results of Ref.14, see its Eqs. (14) and (19).

⁸M. Hasenbusch, *J. Phys. A* **34**, 8221 (2001).

⁹Y. Deng, *Phys. Rev. E* **73**, 056116 (2006).

¹⁰M. Hasenbusch, A. Pelissetto, and E. Vicari, *Phys. Rev. B* **72**, 014532 (2005).

¹¹P. Calabrese, A. Pelissetto, and E. Vicari, *Phys. Rev. B* **67**, 054505 (2003).

¹²A. Aharony, in *Phase Transitions and Critical Phenomena*, edited by C. Domb and J. Lebowitz (Academic, New York, 1976), Vol. 6, p. 357.

¹³M. E. Fisher and D. R. Nelson, *Phys. Rev. Lett.* **32**, 1350 (1974).

¹⁴D. R. Nelson, J. M. Kosterlitz, and M. E. Fisher, *Phys. Rev. Lett.* **33**, 13 (1974); J. M. Kosterlitz, D. R. Nelson, and M. E. Fisher, *Phys. Rev. B* **13**, 412 (1976).

- ¹⁵J. D. Brock, A. Aharony, R. J. Birgeneau, K. W. Evans-Lutterodt, J. D. Litster, P. M. Horn, G. B. Stephenson, and A. R. Tajbaksh, *Phys. Rev. Lett.* **57**, 98 (1986).
- ¹⁶A. Aharony, R. J. Birgeneau, J. D. Brock, and J. D. Litster, *Phys. Rev. Lett.* **57**, 1012 (1986).
- ¹⁷A. Aharony, R. J. Birgeneau, C. W. Garland, Y.-J. Kim, V. V. Lebedev, R. R. Netz, and M. J. Young, *Phys. Rev. Lett.* **74**, 5064 (1995).
- ¹⁸S. R. Andrews and H. Mashiyama, *J. Phys. C* **16**, 4985 (1983).
- ¹⁹G. Helgesen, J. P. Hill, T. R. Thurston, and D. Gibbs, *Phys. Rev. B* **52**, 9446 (1995).
- ²⁰M. P. Zinkin, D. F. McMorrow, J. P. Hill, R. A. Cowley, J.-G. Lussier, A. Gibaud, G. Grübel, and C. Sutter, *Phys. Rev. B* **54**, 3115 (1996).
- ²¹P. Bak, *Phys. Rev. Lett.* **44**, 889 (1980).
- ²²F. J. Wegner, in *Phase Transitions and Critical Phenomena*, edited by C. Domb and M. S. Green (Academic, New York, 1976), Vol. 6.
- ²³J. F. Nicoll, *Phys. Rev. A* **24**, 2203 (1981).
- ²⁴M. Caselle and M. Hasenbusch, *J. Phys. A* **31**, 4603 (1998).
- ²⁵M. De Prato, A. Pelissetto, and E. Vicari, *Phys. Rev. B* **68**, 092403 (2003).
- ²⁶J. M. Carmona, A. Pelissetto, and E. Vicari, *Phys. Rev. B* **61**, 15136 (2000).
- ²⁷P. Pfeuty, D. Jasnow, and M. E. Fisher, *Phys. Rev. B* **10**, 2088 (1974).
- ²⁸J. H. Chen, M. E. Fisher, and B. G. Nickel, *Phys. Rev. Lett.* **48**, 630 (1982); M. E. Fisher and J. H. Chen, *Journal of Physique* **46**, 1645 (1985).
- ²⁹M. Campostrini, M. Hasenbusch, A. Pelissetto, P. Rossi, and E. Vicari, *Phys. Rev. B* **63**, 214503 (2001).
- ³⁰M. Hasenbusch and T. Török, *J. Phys. A* **32**, 6361 (1999).
- ³¹M. Campostrini, A. Pelissetto, P. Rossi, and E. Vicari, *Phys. Rev. E* **60**, 3526 (1999).
- ³²M. Hasenbusch, F. Parisen Toldin, A. Pelissetto, and E. Vicari, *J. Stat. Mech.: Theory Exp.* (2007) P02016.
- ³³P. Calabrese, A. Pelissetto, and E. Vicari, *Phys. Rev. E* **65**, 046115 (2002).
- ³⁴J. D. Brock, D. Y. Noh, B. R. McClain, J. D. Lister, R. J. Birgeneau, A. Aharony, P. M. Horn, and J. C. Liang, *Z. Phys. B* **74**, 197 (1989).
- ³⁵S. Chikazumi, *Physics of Ferromagnetism* (Clarendon, Oxford, 1997), Chap. 12.
- ³⁶D. V. Pakhnin and A. I. Sokolov, *Phys. Rev. B* **61**, 15130 (2000).
- ³⁷R. Folk, Yu. Holovatch, and T. Yavors'kii, *Phys. Rev. B* **62**, 12195 (2000); **63**, 189901(E) (2001).
- ³⁸H. Kleinert and V. Schulte-Frohlinde, *Phys. Lett. B* **342**, 284 (1995).
- ³⁹H. Rohrer and Ch. Gerber, *Phys. Rev. Lett.* **38**, 909 (1977).
- ⁴⁰A. R. King and H. Rohrer, *Phys. Rev. B* **19**, 5864 (1979).
- ⁴¹N. F. Oliveira Jr., A. Paduan Filho, S. R. Salinas, and C. C. Becerra, *Phys. Rev. B* **18**, 6165 (1978).
- ⁴²R. Folk, Yu. Holovatch, and G. Moser, *Phys. Rev. E* **78**, 041124 (2008).
- ⁴³W. Selke, *Phys. Rev. E* **83**, 042102 (2011).
- ⁴⁴U. Wolff, *Phys. Rev. Lett.* **62**, 361 (1989).
- ⁴⁵M. Saito and M. Matsumoto, in *Monte Carlo and Quasi-Monte Carlo Methods 2006*, edited by A. Keller, S. Heinrich, H. Niederreiter (Springer, Berlin, 2008); M. Saito, Masters thesis, Math. Dept., Graduate School of Science, Hiroshima University, 2007. The source code of the program is provided at [<http://www.math.sci.hiroshima-u.ac.jp/~m-mat/MT/SFMT/index.html>].
- ⁴⁶F. Parisen Toldin, *Phys. Rev. E* **84**, 025703 (2011).